Evaluating ephemeral gullies with a process-based topographic index model

Prasad Daggupati, Aleksey Y. Sheshukov, Kyle R. Douglas-Mankin

Published Version Information

Citation: Daggupati, P., Sheshukov, A. Y., & Douglas-Mankin, K. R. (2014). Evaluating ephemeral gullies with a process-based topographic index model. Catena, 113, 177-186.

Digital Object Identifier (DOI): doi:10.1016/j.catena.2013.10.005

Publisher's Link:
http://www.sciencedirect.com/science/article/pii/S034181621300249X

Published in Catena 113 (2014) 177-186 (http://dx.doi.org/10.1016/j.catena.2013.10.005)

Evaluating ephemeral gullies with a process-based topographic index model

Prasad Daggupati[1], Aleksey Y. Sheshukov*, Kyle R. Douglas-Mankin

Department of Biological and Agricultural Engineering, Kansas State University, 129 Seaton Hall, Manhattan, KS, USA

KEYWORDS

Ephemeral gully
Erosion
Sediment
Overland flow
SWAT
Topography

A B S T R A C T

Soil conservation practices have been implemented to control soil degradation from sheet and rill erosion, but excessive sediment runoff remains among the most prevalent water quality problems in the world. Ephemeral gully (EG) erosion has been recognized as a major source of sediment in agricultural watersheds; thus, predicting location and length of EGs is important to assess sediment contribution from EG erosion. Geomorphological models are based on topographic information and ignore other important factors such as precipitation, soil, topography, and land use/land management practices, whereas physically based models are complex, require detailed input information, and are difficult to apply to larger areas. In this study, an approach was developed to incorporate a process-based Overland Flow-Turbulent (OFT) EG model that contained factors accounting for drainage area, surface roughness, slope, soil critical shear stress, and surface runoff in the ArcGIS environment. Two hydrologic models, Soil Water Assessment Tool (SWAT) and ArcCN-Runoff (ACR), were adopted to simulate precipitation excess in Goose Creek watershed in central Kansas, USA. These two realizations of the OFT model were compared with the Slope-Area (SA) topographic index model for accuracy of EG location identification and length calculation. The critical threshold index in the SA model was calibrated in a single field in the watershed prior to EG identification whereas the OFT models were uncalibrated. Results demonstrated overall similar performance between calibrated SA model and uncalibrated OFT-SWAT model, and both outperformed the uncalibrated OFT-ACR model. In simulation of EG location, the OFT-SWAT model resulted in 12% fewer false negatives but 8% more false positives than the SA model, compared with 19% fewer false positive and 6% more false negatives than the OFT-ACR model. Greater errors in runoff estimation by ACR translated directly into errors in EG simulation. All models over-predicted EG lengths compared with observed data, though OFT-SWAT and SA models did so with better fit exceedance probability curves, about zero Nash-Sutcliff model efficiency and ⩽40% bias compared to -3 model efficiency and >100% bias for OFT-ACR. Success of the uncalibrated OFT-SWAT model in producing satisfactory predictions of EG location and EG length shows promise for process-based EG simulation. The OFT-SWAT model used data and parameters also commonly used for SWAT model development, which should simplify its adoption to other watersheds and regions. Further testing is needed to determine the robustness of the OFT-SWAT model to dissimilar field and hydrologic conditions. It is expected that inclusion of more site-specific physical properties in OFT-SWAT would improve model performance in predicting location and length of EGs, which is essential for accurate estimation of EG sediment erosion rates.

1. Introduction

Over the past few decades, various soil conservation practices have been implemented to control soil erosion originating from agricultural fields. The National Resource Inventory on soil erosion from cropland (NRI, 2007) reported a 43% decrease in soil erosion in the United States between 1982 and 2007; regardless, excessive sediment runoff remains among the most prevalent water quality problems in the U.S.A. (Hargrove et al., 2010). Implemented soil conservation practices substantially reduced sheet and rill erosion, but impact on ephemeral gully (EG) erosion is unclear. Recent studies (Foster, 1986; Poesen et al., 1996; Nachtergaele and Poesen, 1999; Poesen et al., 2003; Hargrove et al., 2010; Knapen and Poesen, 2010; Poesen et al., 2011; Daggupati, 2012) have shown that EG erosion is a major contributor of sediment in streams and needs serious attention.

* *Corresponding author*. Tel.: +1 785 532 5418; fax: +1 785 532 5825.
E-mail addresses: pdaggupati@tamu.edu (P. Daggupati), ashesh@ksu.edu (A.Y. Sheshukov), krdmankin@gmail.com (K.R. Douglas-Mankin).
1 Presently at Texas A&M University, College Station, TX 77843, USA.

EGs are concentrated flow channels of various sizes that form mostly along natural drainage lines in agricultural fields when vegetation cover is minimal and runoff energy of water (precipitation excess) exceeds critical shear stress of soil. EGs erode topsoil, but tillage fills them in, often with less-productive subsoil. If not corrected, EGs may grow into permanent gullies.

Soil loss due to EG erosion can contribute about 10% of the total soil loss in small watersheds (Poesen et al., 1996). In actively eroding areas, however, the contribution of EG erosion can range from 30% to as much as 100% of the total soil loss, as reported by Casalí et al. (1999), thus exceeding the contribution of sheet and rill erosion. The contribution of EG erosion varies geographically. In the U.S.A., EG erosion contributed from 17% of total soil loss in New York State to 73% in Washington State (Robinson et al., 2000). In central Belgium, EG erosion accounted for 44% of soil loss (Poesen et al., 1996), whereas in the Mediterranean and southern Portugal regions, EG erosion contributions were as high as 83% (Vandaele et al., 1996b). In the Loess Plateau of China, EG erosion ranged from 41% to 91% of soil loss (Zheng and Gao, 2000).

Four important factors that affect the formation and development of EGs are precipitation, topography, soil, and land use/land management practices. EGs form only after threshold precipitation intensity and duration are attained. Very few studies have investigated threshold precipitation events required for EG formation, and those studies are typically restricted to small areas examined over short time periods (Capra et al., 2009). The threshold precipitation needed for the formation and development of EGs varied geographically depending on soil conditions and initial soil moisture content. Various studies reported the threshold precipitation from 14.5 to 22 mm for cropland. Minimum precipitation depths of 15 mm in winter and 28 mm in summer were needed for the formation of EGs based on a study spanning a 15-year period in central Belgium (Nachtergaele et al., 2001a). Casalí et al. (1999) reported that within the three year period from October 1994 to September 1997, only three rainfall events were able to promote EGs in agricultural fields of Navarra region of Spain: the events with total water depth of 17 mm, 51 mm, and 53 mm and peak precipitation intensity of 54 mm/hr, 12 mm/hr, and 156 mm/hr, respectively. Cerdan et al. (2002) found the precipitation depth of 28.5 mm and maximum 6-minute intensity of 15 mm/hr in December and 21.6 mm depth and 98 mm/hr 6-minute intensity in summer resulted in formation of rill EGs in a cropland area. Capra et al. (2009) observed EG formation for an 8-year period and utilized the factors of antecedent precipitation index, maximum value of 3-day precipitation, and a simple surrogate for soil water content to find out that a threshold of 51 mm for the index was needed for EG formation.

Formation of EGs has been described in the literature as a topographic phenomenon (Patton and Schumm, 1975; Throne et al., 1986; Montgomery and Dietrich, 1994). Topographic attributes such as upstream drainage area (used as surrogate for flow), slope, and plan of curvature are key topographic controls in the formation process. Over the past few decades, these attributes were combined into several indices that have been used to identify locations of EGs (Thorne and Zevenbergen, 1984; Foster, 1986; Vandaele et al., 1996a,b; Desmet et al., 1999; Nachtergaele and Poesen, 1999; Knapen and Poesen, 2010; Daggupati et al., 2013).

Soil (particularly topsoil) resistance to concentrated flow erosion plays an important role in the formation of EGs (Poesen et al., 2003). Knapen et al. (2007) hypothesized that gully initiation at a given location in the landscape is controlled not only hydrologically and topographically but also by erosion resistance of topsoil. Knapen and Poesen (2010) proved their hypothesis using field studies on Belgium loess topsoils. The erosion resistance of topsoil is commonly referred to as soil critical shear stress (τ_{cr}), the threshold at which shearing forces of concentrated water flow initiate soil erosion. Soil critical shear stress is influenced by factors such as soil moisture content, bulk density, particle size distribution, random surface roughness, void space, flow resistance, soil erosivity, surface sealing and crusting, and freezing and thawing (Nearing et al., 1989). Soil critical shear stress values are difficult to define precisely because they vary considerably even for similar soil conditions (Foster, 1986). Few studies reported the values of τ_{cr} that resulted in the formation of EGs: Nachtergaele and Poesen (2002) and Poesen et al. (2003) found that τ_{cr} during peak flow ranged from 3.3 to 32. 2 N/m^2 (mean = 14 N/m^2) for EGs eroded in silt loam (loess-derived) topsoils in Belgium and from 16.8 to 74.4 N/m^2 (mean = 44 N/m^2) for EGs formed in stony sandy loams in Portugal. Poesen at al. (2011) stressed the need to collect and report τ_{cr} values leading to EG formation in a range of environments.

Land use arguably plays the most important role in EG formation. EG forms predominantly in cultivated crop fields where channels can be removed by tillage. Several recent studies have documented that gradual or sudden shifts in land use resulted in triggering of gullying or increased gully erosion rates (Poesen et al., 2011). Field observations in central Belgium showed that an increase in area under maize resulted in increased EG erosion risk (Nachtergaele et al., 2001a, as cited in Poesen et al., 2011). Poesen et al. (2011) stressed the need for more research on the drivers of land use changes causing increased or decreased gully erosion risk. Land cover or vegetative biomass has a direct impact on the formation of EGs. Vandekerckhove et al. (2000) reported that land cover has greater influence than climatic conditions in explaining topographic thresholds for different areas. Land cover affects τ_{cr} directly; i.e., reduction in biomass (either above or below ground) results in lowering the erosion resistance of topsoil, which influences EG formation. Prosser and Slade (1994) demonstrated through flume experiments that increased vegetation cover results in decreased susceptibility of valley floors to gully formation. Plant roots can increase τ_{cr} due to increases in soil cohesion (De Baets et al., 2006, 2007).

Empirical and physically based models have been developed to quantify EG erosion at both field and watershed scales. Woodward (1999) developed a physically based Ephemeral Gully Erosion Model (EGEM) in which locations of EGs and EG length were to be provided by the user. Gordon et al. (2007) addressed limitations of EGEM by revising equations for flow that resulted in a Revised EGEM (REGEM) model and incorporated it as a module within the Annualized Agricultural Non-Point Source Model to add EG erosion prediction to standard sheet and rill erosion. Physically based models require a wide set of input physical parameters and are difficult to apply to larger areas, so simplistic empirical and regression models were developed for EG volume estimates. Nachtergaele et al. (2001a, 2001b) observed strong relationship between EG volume and EG length in the Mediterranean environment using 112 field-measured EGs. The regression relation between volume (V) and length (L) was represented as $V = 0.048\ L^{1.29}$ with the coefficient of determination (R^2) of 0.91. Capra and Scicolone (2002) and Capra et al. (2005) used data from 92 EGs in Italy to derive a relationship $V = 0.0082\ L^{1.42}$ with R^2 of 0.64. Zhang et al. (2007) reported a similar power-function relationship using 21 EGs in northeastern China to yield $V = 0.015\ L^{1.43}$ with an R^2 of 0.67.

Daggupati et al. (2013) used the GIS environment to automate calculation of potential lengths of EGs using various topographic index models and explored model threshold sensitivity. The studied topographic models were simplistic, purely empirical, and utilized a limited set of physical characteristics (Daggupati et al., 2013); on the other hand, physically based models were complex, required large sets of input parameters, and were difficult and time-consuming to apply to larger areas. Therefore, the objectives of this study were (1) to find a middle ground by developing a physically

based model using a GIS framework capable of predicting location and length of EGs and (2) to evaluate performance of the new model on an individual field and in a small watershed.

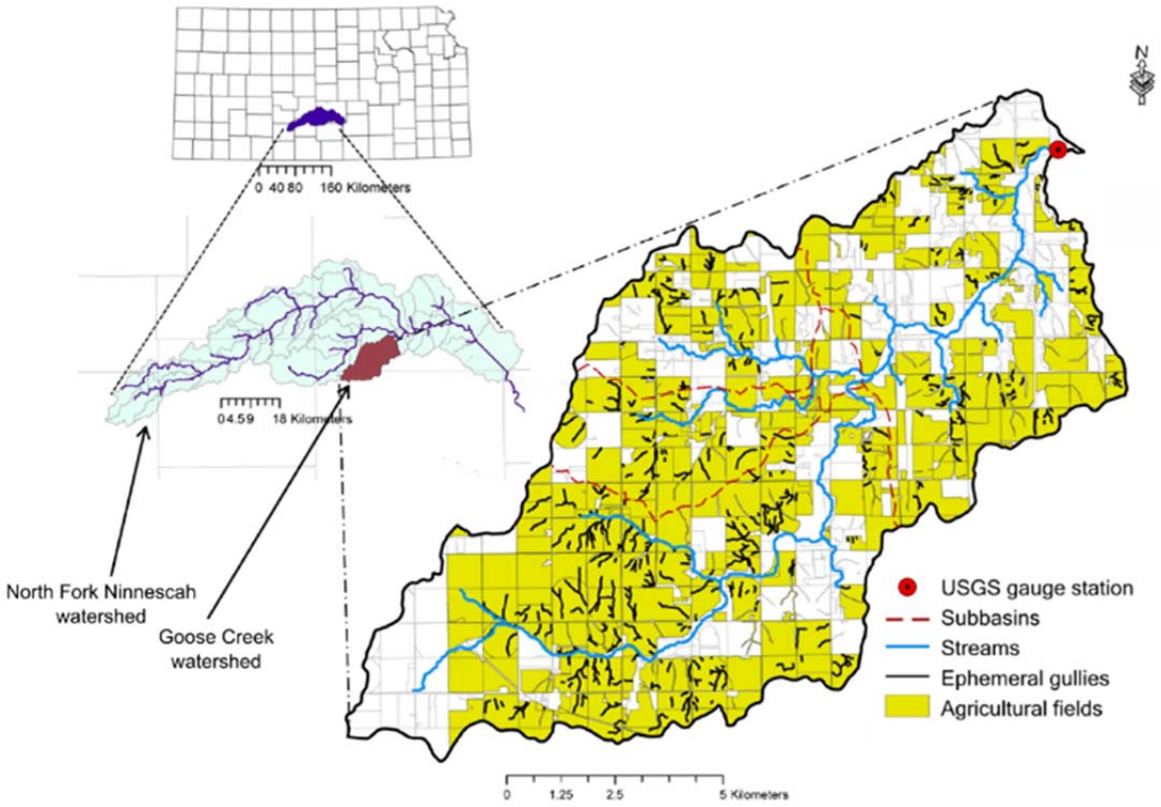

Fig. 1. Map of North Fork Ninnescah watershed and Goose Creek subwatershed in central Kansas. Black lines represent a network of digitized ephemeral gullies within agricultural fields.

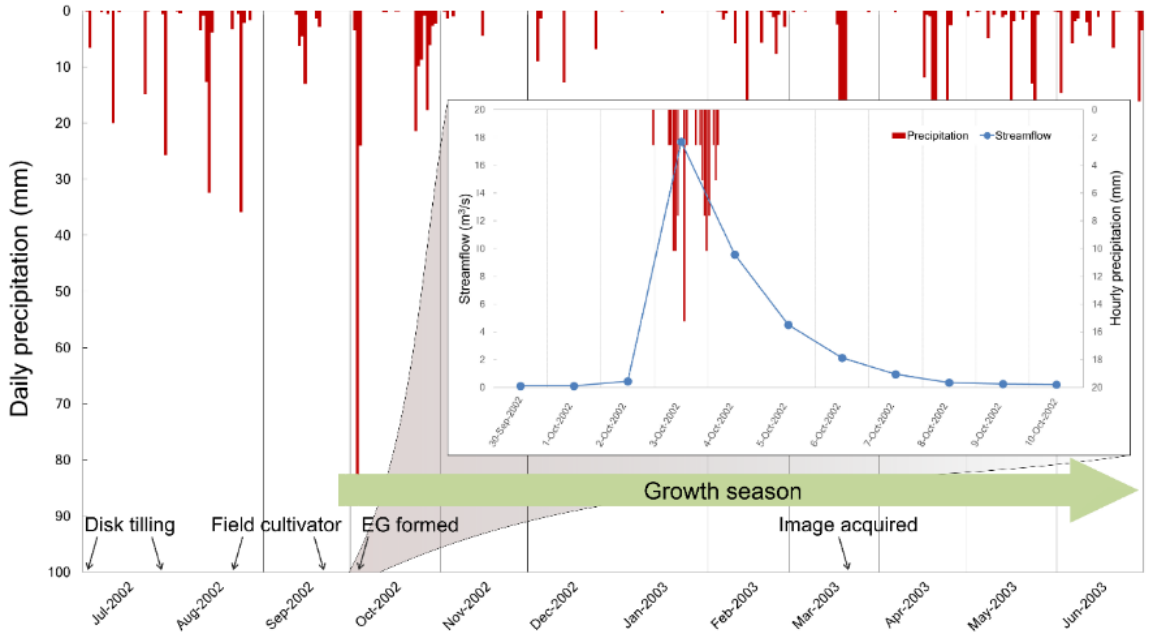

Fig. 2. Timeline from 2002 to 2003 of the wheat growth season, applied management practices, and daily precipitation in the Goose Creek watershed. The inset shows hourly precipitation and daily hydrograph for the EG formation period from 30 September 2002 through 10 October 2002.

2. Study Area

The Goose Creek watershed (12-digit Hydrologic Unit Code [HUC] 110300140204) is a 13,306 ha subwatershed within North Fork Ninnescah watershed (8-digit HUC 11030014) in Reno and Kingman counties of central Kansas, U.S.A., that drains into the North Fork river (Figure 1). Primary land use in the watershed was cropland (64%), followed by rangeland (29%), woodland (6%), and 1% other uses (water, urban). Fine loamy-textured soils highly susceptible to EG erosion were predominant in this watershed (KDHE, 2000; Parajuli et al., 2009). Slopes ranged from 0.0 to 46.1% with a median of 0.9%. The major crop in the watershed was winter wheat, which is typically planted in the fall and harvested in late spring or early summer. The other cultivated crops in the watershed, such as grain sorghum, corn, and soybeans, were warm-season crops. Most cultivated fields in the watershed were conventionally tilled. The nearest land-based weather station was located near the city of Pretty Prairie, Kansas (NCDC USC00146573; Lat: 37.79º, Lon: -98.03º), about 13 km east of the watershed.

Erosion from EGs is a major concern in the watershed (Daggupati et al., 2010; Douglas-Mankin et al., 2011). Preliminary monitoring results as part of a United States Department of Agriculture Conservation Effects Assessment Project (CEAP) showed that EGs in the watershed contributed roughly 2.46 Mg/ha (Douglas-Mankin et al., 2011); an estimated average EG contribution for Kansas was 2.92 Mg/ha, compared with 8.06 Mg/ha from sheet and rill erosion (USDA-NRCS, 1997).

Files must be in MS Word only and should be formatted for direct printing, using the CRC MS Word provided. Figures and tables should be embedded and not supplied separately.

2.1. Assessing Ephemeral Gullies

A period from 2002 to 2003 was selected for this study due to availability of aerial imagery, farmer management scheduling, hourly precipitation data, and daily streamflow data. The majority of cropland in the study area was planted to wheat. Farmers typically complete tilling the land in mid-September and plant wheat during the last week of September (Figure 2; French, 2010, personal communication). A Digital Ortho Quarter Quadrangle aerial image of Goose Creek watershed acquired on 22 March 2003 and published as Google Earth historical imagery (Google, 2010) was used in this study. This image was taken when crop cover (wheat) was not fully established, and, therefore, it visually showed a network of fully developed EGs. In comparison, other historical images published in Google Earth for the study area were acquired during the crop growing season with crop fully established, and hence locating EGs was very difficult. Analysis of hourly precipitation records from the Pretty Prairie weather station showed that EGs visible on the aerial image of 22 March most likely resulted from a series of precipitation events from 2 October through 4 October 2002, with the highest rainfall of 83.5 mm on 3 October (3.5 mm on 2 October and 24.1 mm on 4 October) as illustrated in the inset of Figure 2. Other events after 4 October 2002 and before 22 March 2003 had smaller precipitation depth and canopy was already partially established which reduced favorable conditions for formation of EGs. Additional support for the event on 3 October can be found by looking at stream flow at the watershed outlet that recorded a peak of 17.7 m^3/s on 3 October (Figure 2) compared with much smaller peaks during other events between the wheat planting and aerial image acquisition dates. Because the crop had been planted prior to the event on 3 October, the fields could not be tilled before the aerial image acquisition date to smooth EGs. All the evidence suggest that the storm events on 3 October resulted in high surface runoff that day and led to formation of EGs.

2.2. Digitizing Ephemeral Gullies

EGs in the study area were digitized with extreme care along the trajectory on the aerial image. Starting and ending points of an EG were difficult to determine visually, so a color identification procedure was implemented. In brief, the color of pixels within an EG was white, and pixels within a field were either green, or brown, or grey. During the identification procedure, a starting pixel of EG was recorded when color changed from the field color to white, then white pixels were tracked along the EG trajectory until the color was changed back from white. The Google Earth (Google, 2010) imagery and hill shade raster files created from Digital Elevation Models (DEM; USDA-NRCS, 2011) to enhance the relief of the surface were used to cross check EG occurrence during the digitizing process in ArcGIS (ESRI, 2011). There were 874 EG fields identified with EGs ranged from 14 m to 819 m. In addition to geospatial manipulations, a windshield survey of agricultural fields was conducted by driving a vehicle along public roads in the watershed and verifying existence of digitized EGs. A map of digitized EGs was intended to be used as a reference spatial dataset for comparison with modeling results.

3. Ephemeral Gully Models

3.1. Topographic SA model

Topographic index models use combinations of primary topographic attributes, such as drainage area and local curvature and slope, to calculate an index value at each point (or pixel) of a field. Field locations for which the index exceeds a threshold are determined to have conditions conducive to EG formation (Montgomery and Dietrich, 1994). Due to a sole topographic nature of these models, they do not account for hydrological, land use, soil, or climatic properties and cannot be applied to specific rainfall events.

One topographic index model, the SA model, was proposed by Moore et al. (1988) and uses a product of local slope (S) and upstream drainage area (A) to compose an index T_{SA} as

$$T_{SA} = S \cdot A \qquad (1)$$

An EG is determined to exist at each point (or pixel in DEM) having an index T_{SA} greater than a specified threshold T_{SA}^{cr}. All points within a field that have index exceeded the threshold value contribute to an EG. In Daggupati et al. (2013) the SA model outperformed three other topographic index models; a threshold $T_{SA}^{cr} = 50$ was optimal for identifying location and length of EGs in the Goose Creek watershed. An automated GIS procedure was developed to locate and estimate length of EGs using a series of refinement steps and geospatial manipulations in ArcGIS (ESRI, 2011), and consisted of converting EG raster file to polyline shapefile, snapping disconnected intervals within a polyline, calculating the length of each polyline and eliminating those that are shorter than a given EG threshold, and assigning each polyline to an individual EG catchment thus eliminating multiple EGs in a single drainage area (Daggupati et al., 2013). The SA model was used for comparison against an alternative process-based model discussed in section 3.2.

3.2. Process-based OFT Model

Three processes have been identified as causing EG formation (Montgomery and Dietrich, 1994): (a) overland flow, in which flow exerts a boundary shear stress in excess of critical shear stress; (b) seepage, in which seepage gradients entrain surficial material as a result of water flowing through and emerging from the soil; and (c) land sliding. Most EGs observed during field surveys across the state of Kansas were found to be formed due to overland flow (Daggupati et al., 2010; Douglas-Mankin et al., 2011). In agricultural fields, the overland flow regime is predominantly turbulent because of the imposed roughness after tillage (Prosser and Abernethy, 1996). Montgomery and Dietrich (1994) developed an approach to estimate a critical drainage area for channel erosion initiated by overland flow at any point in the field. The approach assumes steady-state precipitation intensity over a surface with uniform infiltration capacity and evaluates a flow discharge using Manning's equation for flow velocity:

$$q = \frac{1}{n} h^{5/3} S^{1/2} \quad (2)$$

where q is discharge per unit contour length ($m^3/s/m$), h is flow depth (m), n is Manning's roughness coefficient ($s/m^{1/3}$), and S is water surface slope (m/m).

The critical shear stress τ_{cr} (N/m^2) of gully formation is determined by the following equation

$$\tau_{cr} = \rho_w g (hS)_{cr} \quad (3)$$

where ρ_w is density of water (kg/m^3), and g is acceleration due to gravity (m/s^2). Rearranging Eq. (3) to solve for h_{cr}, and substituting it in Eq. (2) yields the critical flow discharge q_{cr} that can be rewritten in a form of index T_{OFT} using a drainage area per unit contour length A_S (m^2/m) and assuming a steady-state precipitation excess rate E (m):

$$T_{OFT} = C\, n (\rho_w g)^{5/3} \tau_{cr}{}^{-5/3} E\, S^{7/6} A_S \quad (4)$$

where C (s/m^3) is the conversion factor. This process-based index model (Eq. (4)) is based on an assumption that EGs form by turbulent overland flow and will be called an Overland Flow-Turbulent (OFT) model. The critical threshold T_{OFT}^{cr} for the OFT model represents the case where drainage area A_S equals the critical drainage area A_{cr} at which EG erosion initiates. An EG forms when $T_{OFT} > T_{OFT}^{cr}$, or A_S is greater than A_{cr}. In Eq. (4), the index T_{OFT} is a function of topographic features (S, A_S), land cover condition (n), weather and hydrology (E), and soil property (τ_{cr}). Physical properties embedded as terms in the index model (Eq. (4)) provide additional information for EG identification and length calculation that were unavailable in the "purely topographic" SA model. Although these features demonstrate additional insight into EG dependency on field characteristics, they also require detailed modeling of hydrologic processes in the field.

3.3. Geospatial Model

An automated GIS procedure to locate and predict the length of EGs was developed for the OFT model (Eq. (4)) using an ArcGIS toolbox builder framework (Figure 3; ESRI, 2011). The procedure followed several steps: (a) The Common Land Unit (CLU) field boundary layer was overlaid with geospatial land-use layer to clip out non-agricultural areas and identify only cropland fields in the watershed. (b) Then for each field, spatial datasets with topography, soil, land use, management, and runoff data were used to calculate an index (Eq. (4)) at each point within the field. (c) Next, the index was compared to a critical threshold value, and all points for which the index exceeded the threshold value were entered in a raster format. (d) Then, similar to the geospatial model developed for the SA model in section 3.1, EGs were located within individual catchments, and EG length was calculated. (e) Finally, statistical analysis of EG occurrence was completed.

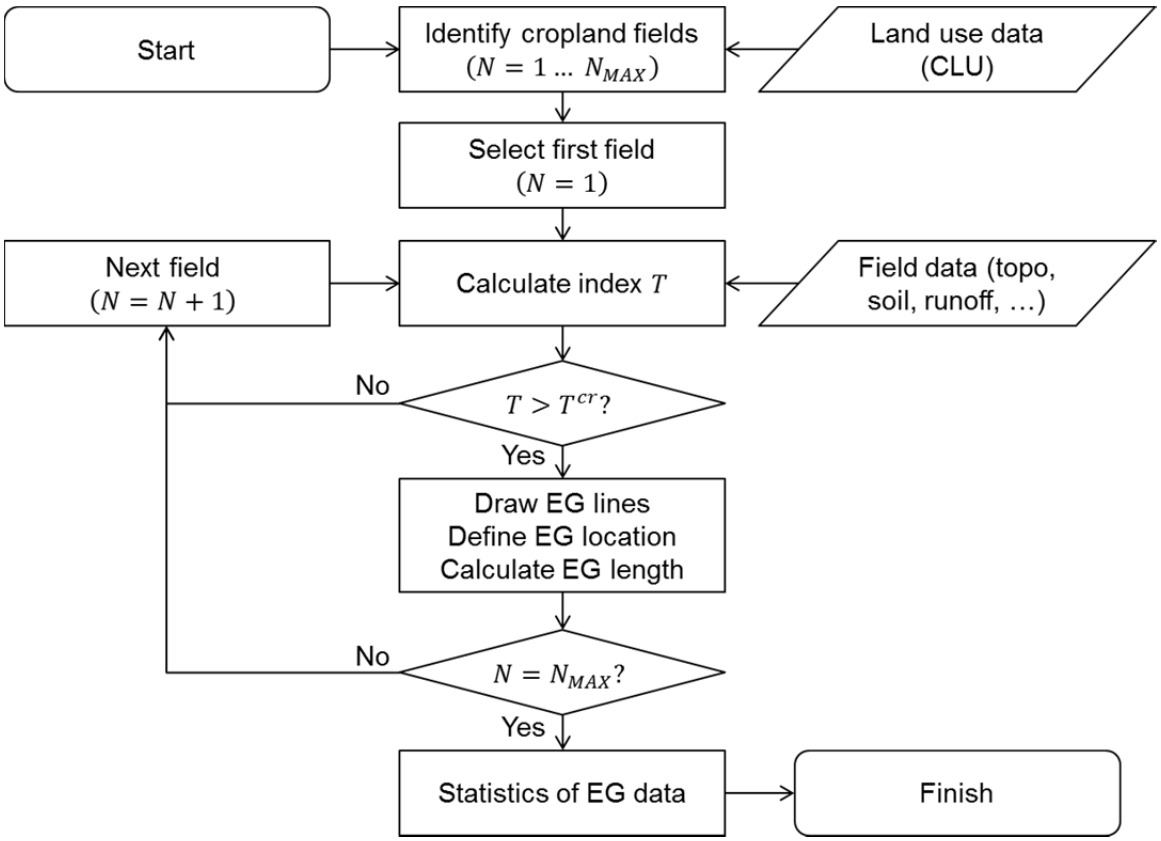

Fig. 3. Flowchart of the geospatial model that identifies location and calculates length of ephemeral gullies in cropland fields.

The topographic parameters were calculated using tools in an ArcGIS toolbox and a deterministic eight-direction (D8) algorithm (O'Callagham and Mark, 1984). An upstream drainage (or catchment) area per unit of contour length was calculated by dividing the drainage area by resolution of the DEM. The soil critical shear stress was calculated based on percentage of clay content (P_c) in topsoil (Smerdon and Beasley, 1961) acquired from the SSURGO database (USDA-NRCS, 2005):

$$\tau_{cr} = 0.311 \cdot 10^{0.00182 P_c} \quad (5)$$

Management practices and amount of land cover affect mechanical properties of topsoil, so τ_{cr} must be adjusted accordingly (Knapen et al., 2007; Souchère et al., 2003; Gordon et al., 2007). In this study, wheat was planted one week prior to the formation of EGs, so the land could be considered bare and τ_{cr} could be left unadjusted in Eq. (5). Value of overland flow roughness coefficient n was 0.03 for wheat cover, and density of water was not adjusted for temperature or impurities.

Precipitation excess depends on many conditions, such as field conditions before and during a precipitation event, soil water content, and rainfall intensity. Two hydrologic models were used to simulate precipitation excess on the day of EG formation: Soil and Water Assessment Tool (SWAT) and ArcCN-Runoff (ACR) tool. SWAT was selected as a widely used model that can provide reasonably accurate, continuous (daily) rainfall-excess runoff simulation in the Midwest U.S.A. ACR was selected as a simple model that is easily implemented in a GIS framework and provides more generalized event-based surface runoff simulation.

4. Hydrologic Models

4.1. SWAT Model

The Soil and Water Assessment Tool (SWAT) model, version 2009 (Arnold et al., 1998; Gassman et al., 2007; Douglas-Mankin et al., 2010), was used as a hydrologic model to simulate runoff on EG fields. The SWAT model divides a watershed into subwatersheds and further into spatially disaggregated hydrologic response units (HRU) based on topography, soil type, and land use and management. SWAT simulates watershed processes on a continuous daily basis and calculates surface runoff for each HRU based on the SCS Curve Number method (USDA-SCS, 1972). The curve number coefficient depends on various factors including hydrologic soil group, land use and land management, and root-zone soil moisture and is updated daily in each HRU (Arnold et al., 2000). SWAT takes daily precipitation datasets as input for each subwatershed in the model.

The SWAT model with 121 subwatersheds and 2,841 HRUs built for the North Fork Ninnescah watershed above Cheney reservoir in Gali et al. (2012) was adopted for this study. Watershed input consisted of topographic 10 m × 10 m DEM (USGS, 1999), SSURGO soil dataset (USDA-NRCS, 2005;

Sheshukov et al., 2011), land use dataset developed from CLU field boundary shapefile, and weather data (Gali et al., 2012). An area of the Goose Creek watershed was represented by 5 subwatersheds and 114 HRUs in the model (Figure 1). Each field was outlined according to field reconnaissance; farming operations were assigned to each field after consulting with Kansas State Research and Extension specialists and according to Devlin et al. (2008). Daily precipitation dataseries from 1 January 1996 to 31 December 2008 were derived for each subwatershed from the Stage III next generation weather radar (NEXRAD) precipitation data available at each 4 km × 4 km grid-cell of the NEXRAD spatial grid network. Each daily dataset was generated by calculating area-weighted average of NEXRAD grid cells intersecting the subwatersheds. Comparing final datasets compiled from NEXRAD data for each subwatershed in the area of Goose Creek watershed with a single daily dataset prepared from hourly data at the Pretty Prairie weather station showed 94% agreement over the period of EG formation from 16 September 2002 to 22 October 2002. This excellent agreement between precipitation datasets supports using the SWAT model with NEXRAD precipitation data for simulating surface runoff in EG fields.

The SWAT model was run from 1 January 1996 to 31 December 2008 with a model spinoff period of 6 years (1996 -2001) and calibrated for streamflow from 2002 through 2008 at the location of the USGS stream gauging station 07144680. A baseflow filter program (Arnold and Allen, 1999) was used to adjust baseflow parameters, whereas other parameters were calibrated according to the procedure presented in Gali et al. (2012). The model agreement with the observed flow data was satisfactory to very good for daily values (Nash-Sutcliffe model efficiency, NSE: 0.47; coefficient of determination, R^2: 0.53; percentage bias, PBIAS: 26.6%), and agreement for monthly values was good to very good (NSE: 0.65; R^2: 0.58; PBIAS: 26.9%) as classified by Moriasi et al. (2007). Daily comparison of observed and modeled stream flow showed that the model captured peaks during summer months with greater accuracy. Because the main interest of this study was in EG formation that generally results from higher flow rate events, an improvement to calibration was not considered necessary.

4.2. ACR Model

A simplified curve number–based ArcCN-Runoff (ACR) tool (Zhan and Huang, 2004), an event-based hydrologic model, was utilized for simulating spatial hydrologic response and surface runoff in EG catchments to a single precipitation event of 83.5 mm on 3 October 2002. Hourly precipitation dataset from the Pretty Prairie weather station was used as model input. The ACR tool is implemented in ArcGIS, and it uses only geospatial soil (SSURGO) and land use (field reconnaissance) datasets as geospatial inputs. To better represent cropland cover on a day of the storm event, the land use layer was modified to represent cropland as fallow and in poor hydrologic condition. After intersecting polygons of soil and land use datasets, the spatially varied curve numbers were assigned for each intersected polygon according to 83.5 mm of daily rainfall. In ACR, the surface runoff is calculated solely based on the SCS Curve Number method. For each EG catchment within a field, the curve number coefficients from all intersected polygons containing in the catchment were extracted to calculate a single area-weighted average curve number for the EG field.

5. Scenarios

Three scenarios were developed using the SA and OFT ephemeral gully models to locate and predict lengths of EGs in the Goose Creek watershed. The first scenario, called the SA scenario, was developed using the SA model. Two other scenarios utilize the OFT model with either SWAT (OFT-SWAT scenario) or ACR (OFT-ACR scenario) for calculating precipitation excess on the day of EG formation.

5.1. SA Scenario

The SA scenario is based on the SA model. The topographic geospatial 2 m × 2 m resolution DEM layer of the studied area (USDA-NRCS, 2011) was used, and an automated GIS procedure (see section 3.1) was adopted to identify EGs and catchments in the entire watershed. Each EG catchment was assumed to contain a single EG comprised of polylines representing individual gullies, and the EG length was calculated as a cumulative length of all polylines within the catchment. The SA scenario used the threshold value T_{SA}=50 in Eq. (1), which was found optimal for use in Goose Creek watershed by Daggupati et al. (2013).

5.2. OFT-SWAT Scenario

In this scenario, the geospatial process-based OFT model based on Eq. (4) was utilized to identify EGs in the watershed, and the SWAT model was used to calculate a steady-state precipitation excess rate *E*. Daily average surface runoff simulated by SWAT on the day of EG formation, 3 October 2002, was collected from all HRUs. To calculate surface runoff for each EG field, the following procedure was implemented: (a) all HRUs that overlay the EG field were identified, (b) area of each such HRU within the EG field was calculated, and (c) SWAT-generated surface runoff from each HRU was used to calculate an area-weighted average surface runoff for the EG field.

The OFT model requires steady-state precipitation excess rate as an input in Eq. (4). To satisfy this requirement, the storm on 3 October 2002 was assumed to be of constant rate for the duration of the event reduced by the time of concentration. Following a rational hydrograph approach (Wanielista et al., 1997), time of concentration provides the time at which the entire HRU area contributes to flow at the outlet (Neitsch et al., 2005). Analyzing time of concentration in all HRUs in a catchment, the longest time of concentration was used to calculate the duration of the steady-state runoff event. By this method, the 18-hour storm duration on 3 October 2002 was reduced to 17.6-hour runoff duration (on average for all catchments in Goose Creek watershed). A steady-state excess rate was then calculated by dividing the catchment surface runoff acquired from the SWAT model by the duration of the runoff event.

5.3. OFT-ACR Scenario

In this scenario, the geospatial OFT model was utilized to identify EGs in the watershed and the ACR model was used to find a steady-state precipitation excess rate E for the single storm event on 3 October 2002. Based on the SSURGO soil dataset and the modified field reconnaissance land use dataset, a geospatial layer was created with unique curve number values and surface runoff rates for each polygon with the unique combination of soil type and land use. Finally, an area-weighted precipitation excess rate was calculated for each EG field similar to the OFT-SWAT scenario that was used as an input in the OFT model.

6. Results and Discussion

6.1. EG Occurrence and Length Analysis of a Watershed

Accuracy of predicting EG occurrence (presence or absence of EG within a specified area) and EG length by the SA and OFT models were assessed using three scenarios. A statistical error matrix method (Gómez-Gutiérrez et al., 2009; Meyer and Martinez-Casosnovas, 1999; Daggupati et al., 2013) was adopted to assess EG occurrence within fields of one hectare area or less in the watershed. The error matrix approach relies on the presence-absence model, where occurrence of EGs is treated as a binary variable: 1 for presence and 0 for absence. Statistics of false positive (predicted: 1, observed: 0), false negative (predicted: 0, observed: 1) and kappa (occurrence statistics) were used to analyze the performance of each scenario (Table 1).

The OFT-ACR scenario was found to have a greater false positive rate (53%), lower false negative rate (12%), and lower kappa (17%) than the OFT-SWAT scenario (34%, 18%, 29%). Lower false positive and higher false negative rates as well as higher kappa for the OFT-SWAT scenario resulted in better overall performance of the OFT-SWAT scenario compared with the OFT-ACR scenario. The SWAT model generated lower precipitation excess rates than the ACR model, resulting in a greater number of predicted EGs in the catchments with no observed EGs, thus higher false positive rates and lower kappa. The topographic-based SA scenario had lower false positive (26%), higher false negative (30%), and comparable kappa statistics (30%) to the OFT-SWAT scenario, which resulted in slightly better overall accuracy of EG prediction for the SA model. In general, the SWAT model identified EGs more accurately than the event-based ACR model when both models were paired with the OFT model. The OFT-ACR scenario performed considerably worse than either of the two other scenarios.

Better performance of the SA scenario likely resulted due to model's prior calibration in a small area of the Goose Creek watershed and identification of the optimal threshold T_{SA}=50 prior to application to the entire watershed. This result shows that initial calibration of the topographic index model in a small area within a watershed followed by its application to a larger area within the same geographical region can result in reasonable model performance. Daggupati et al. (2013) also reported that calibration of the SA model in one area and application in a substantially different geographical region can significantly alter model performance, which indicates that the SA topographic index model requires site-specific calibration to be effective.

The OFT model adopted in both OFT-SWAT and OFT-ACR scenarios was not calibrated. The parameters in definition of T_{OFT} in Eq. (4), such as critical shear stress and roughness coefficient, were taken from their respective databases without adjustment. The τ_{cr} was expressed by the empirical relationship in Eq. (5), with the percentage of clay in the soil from SSURGO dataset and ρ_w and n assumed constant for all agricultural fields. The occurrence statistics of the OFT-SWAT scenario show a reasonably good performance by the OFT model paired with SWAT for precipitation excess rate calculation, particularly since the OFT-SWAT model was not calibrated, although further investigation to reduce uncertainties associated with definition of model physical parameters is warranted.

Length of EGs was calculated for three scenarios and compared for each field against digitized EGs from the aerial image. The predicted EGs shorter than 50 m were removed from analysis due to potential errors in EG trajectory identification. The length of predicted EGs ranged from 50 m to 1253 m for the OFT-SWAT scenario (median length of 176 m; standard deviation of 144 m), to 1626 m for the OFT-ACR scenario (230 m; 204 m), and to 898 m for the SA scenario (141 m; 121 m), however, the longest EG in the aerial image was digitized at 819 m (109 m; 104 m). The number of matching EG fields between the simulated scenarios and the digitized image was calculated at 714 (81.7% out of all digitized EG fields) for OFT-SWAT, 766 (87.6%) for OFT-ACR, and 610 (69.8%) for SA scenarios.

Table 1. EG occurrence statistics for three scenarios.

Statistics	Scenario		
	OFT-SWAT	OFT-ACR	SA
False positive	34%	53%	26%
False negative	18%	12%	30%
Kappa	29%	17%	30%

Table 2. Statistics of predicted EG length by three scenarios versus the EG length digitized from aerial image.

Statistics	Scenario		
	OFT-SWAT	OFT-ACR	SA
R^2	0.50	0.46	0.39
NSE	-0.29	-2.99	0.08
PBIAS (%)	-42.4	-101.1	-18.0

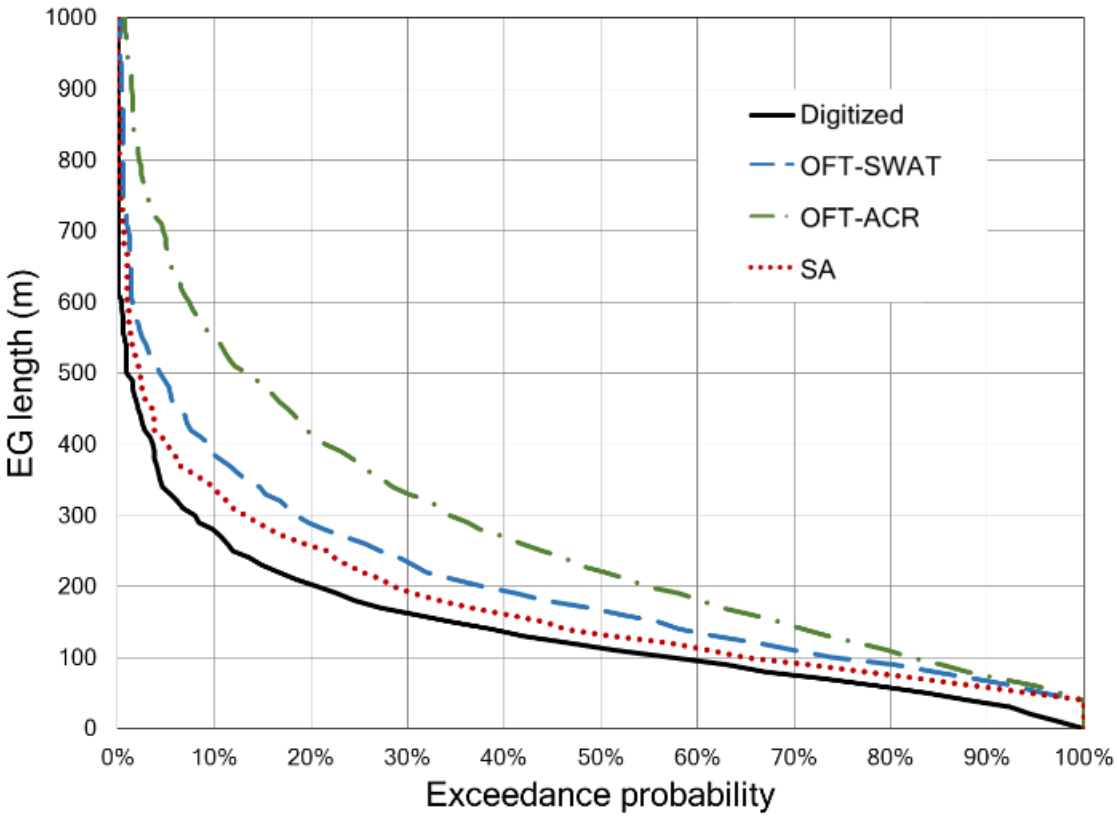

Fig. 4. Exceedance probability curves for lengths of digitized EGs (solid line) and EGs predicted by three scenarios: OFT-SWAT (dash line), OFT-ACR (dash-dotted line), and SA (dotted line).

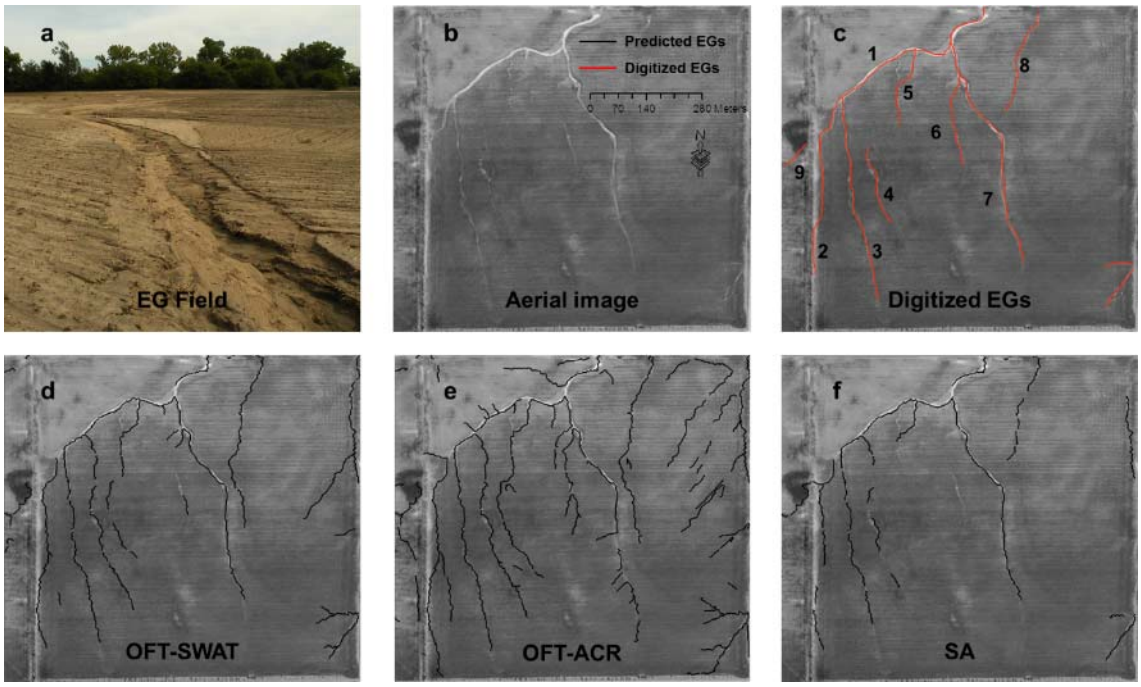

Fig. 5. (a) A picture of ephemeral gullies formed in a one-hectare agricultural field in Goose Creek watershed (taken on 24 October 2009). Observed (b), digitized (c), and predicted (d, e, f) ephemeral gullies resulted from the rainfall event on 3 October 2002.

The comparison statistics (R^2, NSE, and PBIAS) for three scenarios evaluate performance of the models in Table 2. Exceedance probability curves of EG lengths for three simulated and one digitized scenarios were compared in Figure 4. All scenarios exhibited overprediction of EG length, as shown by negative PBIAS values in Table 2 and three scenario curves in Figure 4. The performance of both OFT-SWAT and SA models were considered adequate, with NSE $\approx$ 0.0 and PBIAS $\lesssim$ 40%. The OFT-SWAT model outperformed the SA model by the R^2 statistic, but SA outperformed OFT-SWAT by the NSE and PBIAS criteria. The performance was significantly worse for the OFT-ACR scenario by all statistics. Similar observation can be obtained from Figure 4, where the SA scenario curve was the closest to the digitized EG curve followed by the OFT-SWAT scenario. The difference in EG length from digitized EGs for 50% probability was 15 m for the SA scenario, 50 m for the OFT-SWAT scenario, and 107 m for the OFT-ACR scenario; it increases for longer EGs in a lower exceedance probability range in Figure 4, thus, yielding the OFT-ACR model unreliable. All scenarios generated similar percentage of small EGs for probabilities above 90%, and it was higher than the one from the digitized image because EGs in scenarios were limited by 50 m due to prediction limitation.

A main reason for poor performance of the OFT-ACR scenario was poor estimation of surface runoff by the event-based ACR model. Statistical agreement of the SA model was worse for a whole Goose Creek watershed (Table 2; NSE: 0.08, PBIAS: -18.0%) compared with a small calibration area within it (called S2 in Daggupati et al. (2013); NSE: 0.85, PBIAS: -4.0%). This demonstrates that extrapolation of a calibrated SA topographic index model even to areas in the same geographical area and with similar hydrologic, topographic, soil, and land use conditions can detrimentally impact model performance and should be done with caution.

Similar performance of the uncalibrated OFT-SWAT model to the locally calibrated SA model demonstrates a robustness of the process-based OFT-SWAT model to produce reasonable EG length estimation without calibration. Again, further improvements to the OFT-SWAT model may be possible by reducing uncertainties associated with definition of model physical parameters.

6.2. EG Length Analysis in a Single Field

One agricultural field in the Goose Creek watershed (Figure 5a,b) was selected as a field study area to assess and demonstrate the differences in EG identification and length calculation of the three scenarios (Figure 5d,e,f). A picture of the field (Figure 5a) was taken on 24 October 2009 under the conditions favorable to EG formation and similar to the event occurred on 3 October 2002 and shown on the aerial image in Figure 5b. In that field, wheat was planted in late September 2002, and soil in the area was fine loam (9.5% clay, 27% silt, 63.5% sand) of hydrologic group B.

A map of digitized EGs in Figure 5c shows occurrence of a developed EG on the north side of the field. The EG consisted of two main branches (segments 1 and 7 in Figure 5c) with tributaries 2, 3, 5, and 6. A detachment from the main EG network, segment 4, represents a part of tributary that was removed from the network because of the flow divergence in a low-slope part of the field. Segment 8 is a tributary to segment 1, converging further north at a point not pictured in Figure 5. Segment 2 is a tributary initiated in the ditch along the road. Segment 1 appears to be an EG continuation of segment 9 on the west side of the road. Total length of EG including the main branches 1, 7 and tributaries 2, 3, 5, 6 is 2426 m. The detached segment 4 is 181 m in length. Width of the segment was not estimated.

Analysis of maps produced from three scenarios revealed that the SA scenario underpredicted EG length (1906 m), whereas both OFT scenarios overpredicted length (2739 m in OFT-SWAT and 3030 m in OFT-ACR). In the SA scenario, main field channels 1 and 7 were clearly present, but tributaries were either shortened (segment 5), had discontinued paths (segments 2, 3, 4), or were undetected (segment 6); thus, the length was reduced by 520 m (Figure 5f). The OFT-ACR scenario generated an abundance of ghost channels and extended the tributaries to longer lengths (Figure 5e). The behavior was similar to lowering the threshold T in the index models, thus allowing smaller drainage areas to produce eroded channels. The OFT-SWAT scenario exhibited the most realistic detection of EGs in the field (Figure 5d), but it still predicted more channels than in the digitized aerial image in Figure 5c: segment 4 was connected to the main EG (segment 1), and segments 4, 5 and 8 were overextended. Interestingly, the SA scenario exhibited a good length prediction even though it utilized an approach that relied on field topography only, whereas the OFT-ACR scenario incorporated soil properties and hydrology and performed poorly.

For the field in Figure 5, the difference in precipitation excess rates calculated by ACR and SWAT hydrologic models in the OFT scenarios led to different EG length estimations. An area-weighted average daily surface runoff by the SWAT model was calculated as 29.3 mm, causing an excess rate of 1.62 mm/hr, but it was found to be 47.5 mm by the event-based ACR tool, leading to the precipitation excess rate of 2.63 mm/hr (about 1.5 times higher). The SWAT model updated the curve number daily based on the soil moisture condition, thus incorporating an "actual" soil infiltrating capacity on the day of rainfall event, whereas the curve number in the ACR tool was arbitrarily dependent on soil type and land cover. A lower curve number in the OFT-SWAT scenario generated more infiltration and less surface runoff, which lowered the index T_{OFT} in Eq. (4). This result showed the clear advantage of using models with better representation of physical processes such as in the OFT-SWAT scenario compared with the simplistic topographic index SA model or limited field information in OFT-ACR scenario.

7. Conclusions

Ephemeral gullies on cultivated croplands are major sources of soil erosion and sediment transport to water bodies. Predicting their occurrence and geometric properties, such as length and cross-sectional profile, is important for soil conservation and water-quality assessment. In this study, the process-based OFT model was developed within the ArcGIS framework to locate EG occurrence and length. The model is advancement to a topographic index model because it incorporates physical properties of a specific field through turbulent overland flow equation, such as, topography, precipitation excess, critical soil shear stress, and surface roughness. The precipitation excess is related to a certain rainfall event, whereas the other physical parameters in the model can be acquired from common soil and geographic databases in the U.S.A.

Two hydrologic models, SWAT and ArcCN-Runoff, were selected as two alternatives to simulate the precipitation excess. These two variants of the OFT model were applied in Goose Creek watershed, an agricultural watershed in Central Kansas, where an analysis of precipitation and streamflow

discharge records, visual imagery, and GIS manipulations with DEM layers were conducted to assess and originate locations and calculate length of ephemeral gullies. The SA topographic index model was also applied in the same watershed for comparison.

Visual analysis of the observed fields in the study watershed and statistics developed from EG occurrence and length analysis revealed that the OFT model with precipitation excess from SWAT (scenario OFT-SWAT) performed considerably better than the OFT model with the ArcCN-Runoff tool (scenario OFT-ACR). The fixed value of the CN coefficient in the ACR tool for all fields in the watershed compared to the one adjusted daily in SWAT forced inaccurate (higher) precipitation excess and thereby inaccurate prediction of longer EGs. The OFT model with SWAT slightly overpredicted the EG lengths compared with the observed data, mainly due to uncertainties in estimating lumped physical parameters, such as τ_{cr} and the assumption of a steady-state runoff.

The EG occurrence and length statistics showed that the calibrated SA topographic index model (scenario SA) predicted EGs similar to the uncalibrated OFT-SWAT process-based model, showing that even an incorporation of basic physical processes contributing to overland flow, soil erosion, and sediment detachment on EG fields can offset an extensive and time-consuming calibration process, including field surveying, GIS manipulation, and model calibration.

The OFT model was implemented exclusively with data and parameters that are used for SWAT model development, which should simplify its adoption to other watersheds and regions. Success of the OFT-SWAT model in this watershed without calibration is promising, but further testing is needed to determine the robustness of the OFT-SWAT model to dissimilar field and hydrologic conditions.

It is expected that performance of the physically based, but fairly simplistic, OFT-SWAT model in both location and length simulations would be improved by use of more site-specific values in model parameterization. In addition, success with this fairly simple process-based model provides an indication that other process-based model formulations may be possible that include both greater resolution and accuracy.

Acknowledgements

This material is based on work supported by the USDA National Institute of Food and Agriculture (NIFA) under Agreement No. 2011-51130-31128. This is contribution number 13-284-J from the Kansas Agricultural Experiment Station, Manhattan, Kan., USA. The authors thank Dr. Phil Barnes for discussions and valuable comments regarding ephemeral gully formation processes, and Lisa French and Howard Miller at Cheney Lake Watershed, Inc. for assisting with gully data collection.

REFERENCES

Arnold, J.G., Srinivasan, R., Muttiah, R.S., Williams, J.R., 1998. Large area hydrologic modeling and assessment Part I: Model development. J. American Water Resour. Assoc. 34(1), 73–89.

Arnold, J.G., Allen, P.M., 1999. Automated methods for estimating baseflow and ground water recharge from streamflow records. J. American Water Resour. Assoc. 35(2), 411–424.

Arnold, J. G., Muttiah, R. S., Srinivasan, R., Allen, P. M., 2000. Regional estimation of base flow and groundwater recharge in the Upper Mississippi River Basin. J. Hydrol. 227, 21–40.

Capra, A., Scicolone, B., 2002. Ephemeral gully erosion in a wheat-cultivated area in Sicily, Italy. Biosyst. Eng. 83(1), 119–126.

Capra, A., Mazzara, L. M., Scicolone, B., 2005. Application of the EGEM model to predict ephemeral gully erosion in Sicily (Italy). Catena 59(2), 133–146.

Capra, A., Porto, P., Scicolone, B., 2009. Relationships between rainfall characteristics and ephemeral gully erosion in a cultivated catchment in Sicily (Italy). Soil Till. Res. 105, 77–87.

Casalí, J., López, J. J., Giráldez, J. V., 1999. Ephemeral gully erosion in southern Navarra (Spain). Catena 36(1-2), 65–84.

Cerdan, O., Le Bissonnai, Y., Couturier, A., Bourennane, H., Souchere, V., 2002. Rill erosion on cultivated hillslopes during two extreme rainfall events in Normandy, France. Soil Tillage Res. 67, 99–108.

Daggupati, P., Douglas-Mankin, K.R., Sheshukov, A.Y., Barnes, P.L., 2010. Monitoring and estimating ephemeral gully erosion using field measurements and GIS. ASABE Paper No. 10-9663. ASABE, St. Joseph, MI.

Daggupati, P., 2012. GIS methods to implement sediment best management practices and locate ephemeral gullies. Ph.D. Dissertation, Department of Biological and Agricultural Engineering, Kansas State Univ., Manhattan, Kan., USA. 161 pp. Available at: http://krex.k-state.edu/dspace/handle/2097/13522.

Daggupati, P., Douglas-Mankin, K.R., Sheshukov, A.Y., 2013. Predicting ephemeral gully location and length using topographic index models. Trans. ASABE 56(4), 1427–1440.

De Baets, S., Poesen, J., Gyssels, G., Knapen, A., 2006. Effects of grass roots on the erodibility of topsoils during concentrated flow. Geomorphology 76, 54–67.

De Baets, S., Poesen, J., Knapen, A., Galindo, P., 2007. Impact of root architecture on the erosion-reducing potential of roots during concentrated flow. Earth Surf. Proc. Land. 32, 1323–1345.

Desmet, P. J. J., Poesen, J., Govers, G., Vandaele, K., 1999. Importance of slope gradient and contributing area for optimal prediction of the initiation and trajectory of ephemeral gullies. Catena 37, 377–392.

Devlin, D., Nelson, N., French, L., Miller, H., Barnes, P. L., Frees, L., 2008. Cheney Lake watershed: Conservation practice implementation history and trends. EP-157, Kansas State Univ., Manhattan, Kan., USA. Available at: http://www.ksre.ksu.edu/bookstore/pubs/EP157.pdf.

Douglas-Mankin, K. R., Srinivasan, R., Arnold, J. G., 2010. Soil and Water Assessment Tool (SWAT) model: Current developments and applications. Trans. ASABE. 53(5), 1423–1431.

Douglas-Mankin, K., Daggupati, P., Sheshukov, A., Barnes, P., Devlin, D., Nelson, N., 2011. Cheney Lake watershed: Erosion from ephemeral gullies. MF-3030, Kansas State Research and Extension, Manhattan, Kan., USA. Available at: http://www.ksre.ksu.edu/bookstore/pubs/MF3030.pdf.

ESRI, 2011. ArcMap 10. Environmental Systems Resource Institute. Redlands, California.

Foster, G. R., 1986. Understanding ephemeral gully erosion. Soil Conservation, Vol. 2. National Academy of Science Press, Washington, DC, pp. 90–125.

French, L., 2010. Cheney Lake Watershed Inc., (personal communication).

Gali, R. K., Douglas-Mankin, K. R., Li, X., Xu, T., 2012. Assessing NEXRAD P3 Data effects on stream-flow simulation using SWAT model in an agricultural watershed. J. Hydrol. Eng. 17(11), 1245–1254.

Gassman, P. W., Reyes, M. R., Green, C. H., Arnold, J. G., 2007. The Soil and Water Assessment Tool: Historical development, applications, and future research directions. Trans. ASABE. 50(4), 1211–1250.

Gordon, L. M., Bennett, S. J., Bingner, R. L., Theurer, F. D., Alonso, C. V., 2007. Simulating ephemeral gully erosion in AnnAGNPS. Trans. ASABE. 50(3), 857–866.

Google, 2010. Google Earth, Version 5.1.3533.1731. Available at http://www.google.com/earth/index.html.

Gómez-Gutiérrez, A., Schnabel, S., Felicısimo, A. M., 2009. Modelling the occurrence of gullies in rangelands of southwest Spain. Earth Surf. Proc. Land. 34(14), 1894–1902.

Hargrove, W. L., Johnson, D., Snethen, D., Middendorf, J., 2010. From dust bowl to mud bowl: sedimentation, conservation measures, and the future of reservoirs. J. Soil Water Cons. 65(1), 14A–17A.

KDHE, 2000. A Watershed Conditions Report for the State of Kansas HUC 11030014 (North Fork Ninnescah). Kansas Department of Health and Environment: Topeka, Kan., USA. Available at: http://www.kdheks.gov/nps/wc_reports/11030014.pdf.

Knapen, A., Poesen, J., Govers, G., 2007. Resistance of soils to concentrated flow erosion: A review. Earth-Sci. Rev. 80, 75–109.

Knapen, A., Poesen, J., 2010. Soil erosion resistance effects on rill and gully initiation points and dimensions. Earth Surf. Process. Land. 35, 217–228.

Meyer, A., Martinez-Casasnovas, J. A., 1999. Prediction of existing gully erosion in vineyard parcels of the NE Spain: A logistic modelling approach. Soil Tillage Res. 50 (3–4), 319–333.

Montgomery, D. R., Dietrich, W.E., 1994. Landscape dissection and drainage area-slope thresholds. In: Process Models and Theoretical Geomorphology, M. J. Kirby (Ed.). Wiley, New York, pp. 221–246.

Moore, I. D., Burch, G. J., Mackenzie, D. H., 1988. Topographic effects on the distribution of surface soil water and the location of ephemeral gullies. Trans. ASAE 32, 1098–1107.

Moriasi, D. N., Arnold, J. G., Van Liew, M.W., Bingner, R. L., Harmel, R. D., Veith, T. L., 2007. Model evaluation guidelines for systematic quantification of accuracy in watershed simulations. Trans. ASABE 50(3), 885–900.

Nachtergaele, J., Poesen, J., 1999. Assessment of soil losses by ephemeral gully erosion using high-altitude (stereo) aerial photographs. Earth Surf. Proc. Land. 24(8), 693–706.

Nachtergaele, J., Poesen, J., Vandekerckhove, L., Wijdenes, D. O., Roxo, M., 2001a. Testing the ephemeral gully erosion model (EGEM) for two Mediterranean environments. Earth Surf. Proc. Land. 26, 17–30.

Nachtergaele, J., Poesen, J., Steegen, A., 2001b. The value of a physically based model versus an empirical approach in the prediction of ephemeral gully erosion for loess-derived soils. Geomorphology 40, 237–252.

Nachtergaele, J., Poesen, J., 2002. Spatial and temporal variations in resistance of loess-derived soils to ephemeral gully erosion. Eur. J. Soil Sci. 53, 449–463.

Nearing, M. A., Foster, G. R., Lane, L. J., Finkner, S. C., 1989. A process-based soil erosion model for USDA-Water Erosion Prediction Project technology. Trans. ASAE 32(5), 1587–1593.

Neitsch, S. L., Arnold, J. G., Kiniry, J. R., Williams, J. R., 2005. Soil and Water Assessment Tool (SWAT), Theoretical documentation. Temple, Tex., USA: USDA-ARS Grassland Soil and Water Research Laboratory.

NRI, 2007. Annual National Resources Inventory, Soil Erosion. United States Department of Agriculture, National Resources Conservation Service. Washington, DC.

O'Callagham, J. F., Mark, D. M., 1984. The extraction of drainage networks from digital elevation data. Comput. Vision Graph. 28, 323–344.

Parajuli, P. B., Nelson, N. O., Frees, L. D., Mankin, K. R., 2009. Comparison of AnnAGNPS and SWAT model simulation results in USDA-CEAP agricultural watersheds in south-central Kansas. Hydrol. Process. 23, 748–763.

Patton, P. C., Schumm, S. A., 1975. Gully erosion, northwestern Colorado: a threshold phenomenon. Geology 3(2), 88–90.

Poesen, J., Boardman, J., Wilcox, B., Valentin, C., 1996. Water erosion monitoring and experimentation for global change studies. J. Soil Water Conserv. 51(5), 386–390.

Poesen, J., Nachtergaele, J., Verstraeten, G. Valentin, C., 2003. Gully erosion and environmental change: Importance and research needs. Catena 50, 91–133.

Poesen, J., Torri, D., Vanwalleghem, T., 2011. Ch. 19 – Gully erosion: procedures to adopt when modelling soil erosion in landscapes affected by gullying. In: Morgan, R.P.C., and M.A. Nearing (Eds). Handbook of Erosion Modelling. Oxford, U.K.: Blackwell-Wiley.

Prosser, I. P., Slade, C. J. 1994., Gully formation and the role of valley-floor vegetation, southeastern Australia. Geology 22, 1127–1130.

Prosser, I. P., Abernethy, B. 1996., Predicting the topographic limits to a gully network using a digital terrain model and process thresholds. Water Resour. Res. 23(7), 2289–2298.

Robinson, K. M., Bennett, S. J., Casalí, J., Hanson, G. J., 2000. Processes of headcut growth and migration in rills and gullies. Intl. J. Sediment Res. 15, 69–82.

Sheshukov, A.Y., Daggupati, P., Douglas-Mankin, K. R., Lee, M.-C., 2011. High spatial resolution soil data for watershed modeling: 1. Development of a SSURGO-ArcSWAT utility. J. Natural & Environ. Sci. 2(2), 15–24.

Smerdon, E. T., Beasley, R. P., 1961. Critical tractive forces in cohesive soils. Agr. Eng. 42(1), 26–29.

Souchère, V., Cerdan, O., Ludwig, B., Le Bissonnais, Y., Couturier, A., Papy, F., 2003. Modeling ephemeral gully erosion in small cultivated catchments. Catena 50(2-4), 489–505.

Thorne, C. R., Zevenbergen, L. W., 1984. On-site prediction of ephemeral gully erosion. Report to the U.S. Department of Agriculture, Agricultural Research and Soil Conservation Services.

Thorne, C. R., Zevenbergen, L. W., Grissinger, E. H., Murphey, J. B., 1986. Ephemeral gullies as sources of sediment. Proc. Fourth Federal interagency Sed. Conf. Las Vegas, NV, pp. 3.152–3.161.

USDA-NRCS, 1997. America's private land, a geography of hope. USDA Natural Resources Conservation Service. Washington, D.C.

USDA-NRCS, 2005. Soil Survey Geographic (SSURGO) database. Washington, D.C.: USDA Natural Resources Conservation Service. Available at: http://soildatamart.nrcs.usda.gov/default.aspx.

USDA-NRCS, 2011. Digital Elevation Model Database. USDA Natural Resources Conservation Service. Washington, D.C.

USDA-SCS, 1972. National Engineering Handbook, Hydrology Chapter 4. Washington, D.C.: U.S. Department of Agriculture, Soil Conservation Service.

USGS, 1999. DASC data catalog. Lawrence, Kans.: Kansas Data Access and Support Center. Available at: http://www.kansasgis.org/catalog/catalog.cfm.

Vandaele, K., Poesen, J., Govers, G., van Wesemael, B., 1996a. Geomorphic threshold conditions for ephemeral gully incision. Geomorphology 16, 161–173.

Vandaele, K., Poesen, J., Marques da Silva, J. R., Desmet, P., 1996b. Rates and predictability of ephemeral gully erosion in two contrasting environments. Geomorphologie: Relief, Processus, Environ. 2, 83–96.

Vandekerckhove, L., Poesen, J., Wijdenes, D. O., 2000. Thresholds for gully initiation and sedimentation in Mediterranean Europe. Earth Surf. Proc. Land. 25, 1201–1220.

Wanielista, M., Kersten, R., Eaglin, R., 1997. Hydrology, water quality and quality control. Second Ed. John Wiley & Sons, Inc., New York.

Woodward, D. E., 1999. Method to predict cropland ephemeral gully erosion. Catena 37, 393–399.
Zhan, X., Huang, M. N., 2004. ArcCN-Runoff: An ArcGIS tool for generating curve number and runoff maps. Environ. Modell. Softw. 875–879.
Zhang, Y., Wu, Y., Liu, B., 2007. Characteristics and factors controlling the development of ephemeral gullies in cultivated catchments of black soil region, Northeast China. Soil Tillage Res. 96, 28–41.
Zheng, F., Gao, X., 2000. Process and modeling of soil erosion on loess slope. Shaanxi People's Press, Xi'an, pp. 96–119 (in Chinese).